

Bright flash response recovery of mammalian rods in vivo is rate limited by RGS9

Gabriel Peinado Allina,¹ Christopher Fortenbach,¹ Franklin Naarendorp,⁴ Owen P. Gross,¹ Edward N. Pugh Jr.,^{1,2,3} and Marie E. Burns^{1,2,3}

¹Center for Neuroscience, ²Department of Ophthalmology and Vision Science, and ³Department of Cell Biology and Human Anatomy, University of California, Davis, Davis, CA 95618

⁴Department of Psychology, Northeastern University, Boston, MA 02115

The temporal resolution of scotopic vision is thought to be constrained by the signaling kinetics of retinal rods, which use a highly amplified G-protein cascade to transduce absorbed photons into changes in membrane potential. Much is known about the biochemical mechanisms that determine the kinetics of rod responses *ex vivo*, but the rate-limiting mechanisms *in vivo* are unknown. Using paired flash electroretinograms with improved signal-to-noise, we have recorded the amplitude and kinetics of rod responses to a wide range of flash strengths from living mice. Bright rod responses *in vivo* recovered nearly twice as fast as all previous recordings, although the kinetic consequences of genetic perturbations previously studied *ex vivo* were qualitatively similar. *In vivo*, the dominant time constant of recovery from bright flashes was dramatically reduced by overexpression of the RGS9 complex, revealing G-protein deactivation to be rate limiting for recovery. However, unlike previous *ex vivo* recordings, dim flash responses *in vivo* were relatively unaffected by RGS9 overexpression, suggesting that other mechanisms, such as calcium feedback dynamics that are strongly regulated by the restricted subretinal micro-environment, act to determine rod dim flash kinetics. To assess the consequences for scotopic vision, we used a nocturnal wheel-running assay to measure the ability of wild-type and RGS9-overexpressing mice to detect dim flickering stimuli and found no improvement when rod recovery was speeded by RGS9 overexpression. These results are important for understanding retinal circuitry, in particular as modeled in the large literature that addresses the relationship between the kinetics and sensitivity of retinal responses and visual perception.

INTRODUCTION

The sensitivity and kinetics of the visual system as a whole is thought to be strongly constrained by the sensitivity and kinetics of photoreceptor cells themselves (Hecht et al., 1942). Rod photoreceptors use a highly amplifying G-protein cascade to transduce the absorption of single photons into sizable electrical responses, but they achieve this extraordinary sensitivity at the cost of speed. The slow recovery (exponential time constant, $\tau \sim 200$ ms) of the mouse rod's single-photon response *ex vivo* is speeded by increasing the expression level of the RGS9 complex, indicating that G-protein deactivation is the slowest step in photoresponse recovery (Krispel et al., 2006). G-protein deactivation likewise determines the temporal resolution across the rod synapse (Fortenbach et al., 2015) and possibly beyond (Nishiguchi et al., 2004; Umino et al., 2012; Umino and Solessio, 2013).

Although the *ex vivo* suction electrode recording from mouse rods has revealed the biochemical steps underlying the photoresponse, it nonetheless requires removing the retina from the eye and slicing it into pieces. Such treatment disrupts the native physiological envi-

ronment of the cells and precludes the possibility of studying complex processes such as photoreceptor adaptation on extended timescales or at light intensities that more realistically simulate diurnal variations and produce substantial bleaching of visual pigment. Furthermore, different external media (variants of Ames' and Locke's) have been used for *ex vivo* retinal physiology experiments, and photoreceptor responses in these two media exhibit quite different kinetics. Specifically, the dim flash responses of rods recorded in Locke's medium exhibit a time to peak of ~ 120 ms, whereas those recorded in Ames are markedly slower (Gross and Burns, 2010; Azevedo and Rieke, 2011). As the composition of the fluid in the subretinal space is not well defined, it has been unclear which medium better mimics the conditions in which photoreceptors signal *in vivo*. Given these considerations, it is clear that *in vivo* measurements are critical for determining how the time course of rod signaling impacts the dynamic properties of scotopic vision.

In this study, we used mice with accelerated rod response recovery *ex vivo* (Krispel et al., 2006) to test the

Correspondence to Marie E. Burns: meburns@ucdavis.edu

Abbreviations used: CSF, contrast sensitivity function; ERG, electroretinogram; GCAP, guanylate cyclase-activating protein; PDE, phosphodiesterase; OS, outer segment.

© 2017 Peinado Allina et al. This article is distributed under the terms of an Attribution-Noncommercial-Share Alike-No Mirror Sites license for the first six months after the publication date (see <http://www.rupress.org/terms/>). After six months it is available under a Creative Commons License (Attribution-Noncommercial-Share Alike 4.0 International license, as described at <https://creativecommons.org/licenses/by-nc-sa/4.0/>).



idea that the temporal resolution of scotopic vision is determined by the kinetics of rod signaling. Using a paired flash paradigm of electroretinogram (ERG) recordings with substantially improved signal-to-noise, we recorded the time course of rod dim flash responses *in vivo*. In addition, we adapted the nocturnal wheel-running threshold assay (Naarendorp et al., 2010) to measure temporal contrast sensitivity of the mice under conditions in which rods respond to both increments and decrements of intensity. These methods allowed us to test the hypothesis that the kinetic limitations of the rod responses could account for the behaviorally measured temporal resolution of scotopic vision.

MATERIALS AND METHODS

Animals

All mice were cared for and handled with approval of the University of California, Davis, Institutional Animal Care and Use Committee and in accordance with National Institutes of Health Guidelines. Adult mice (2–4 mo) of WT (C57Bl6/J; The Jackson Laboratory), RGS9-overexpressing (line 2, aka R9AP138; Krispel et al., 2006) and guanylate cyclase-activating proteins^{-/-} (GCAPs^{-/-}; Mendez et al., 2001) strains were housed in a 12:12-h dark/light cycle and dark-adapted overnight for a minimum of 8 h before recording. Under dim red light, mice were anesthetized with isoflurane (1.5%) and positioned on a regulated heating pad that maintained a core temperature of 37°C. A mixture of phenylephrine and tropicamide (2:1) was applied to the corneal surface to achieve mydriasis, after which the eyelids were gently pulled open to induce proptosis, with the purpose of increasing the resistance between the corneal and ground electrodes. Methylcellulose was applied to maintain corneal moisture during the recording.

ERG recordings and illumination system

A Ganzfeld ERG system (Phoenix Research Labs) was used for light stimulation and electrical recording. This apparatus uses Maxwellian view optics to focus the incoming light to a point in the anterior of the eye, creating a homogeneous illumination of the surface of the sensory retina. Correct alignment of the apparatus with respect to the pupil and optics is facilitated by an infrared-sensitive camera and infrared illumination system built into the optics. Electrical contact with the cornea is achieved by a conducting ring through which light passes at the tip of the Maxwellian lens. Substantial improvement in signal amplitude was achieved by minimizing the conducting gel outside the conducting ring. A subepidermal needle placed on the forehead was used as a ground electrode.

To measure the rod photoresponse *in vivo*, we used the paired flash paradigm (Birch et al., 1995; Lyubarsky and

Pugh, 1996; Pepperberg et al., 1997; Hetling and Pepperberg, 1999). In this paradigm, a relatively dim “test” flash is delivered to the eye to generate a subsaturating, transient rod response, followed after various delays by an intense “probe” flash that completely suppresses all remaining rod circulating current. The test flash was generated by a 1-ms pulse from a green LED (peak emission 510 nm), whereas the probe flash was generated by a 1-ms pulse from a UV LED (peak emission 360 nm).

To improve the extraction of the probe flash *a*-wave amplitude in the paired flash protocol, the response to the test flash alone was numerically subtracted from the response to the (test + probe) flash pair to isolate the response of probe flash (Fig. 1 A). To deal with small changes in circulating current that could occur over the time course of the experiment, the maximum *a*-wave amplitude (a_{\max}) in response to the probe flash was measured after an appropriate period of dark adaptation approximately every 10 min. The expected value of a_{\max} at any intervening time point was then calculated by interpolation, and the interpolated value was used to normalize the *a*-wave amplitude in response to the probe flash delivered at various times after a test flash. An experiment was discarded if the a_{\max} was <700 μ V or if the amplitude decreased by >10% over the recording epoch. All data were acquired with the commercial LabScribe2ERG interface provided with the Phoenix Ganzfeld apparatus and subsequently exported to Igor Pro (WaveMetrics) for analysis with custom scripts.

The duration and the total number of photons generated by the LEDs for all stimuli were measured using a high-speed photodiode (UDT Instruments) and calibrated neutral density filters. To calculate the number of photoisomerizations elicited per rod, the number of photons delivered by a flash was divided by a retinal surface of 18 mm² and multiplied by an end-on collecting area of 0.87 μ m² (Lyubarsky et al., 2004).

Behavioral experiments and analysis

The mouse nocturnal wheel-running assay (Naarendorp et al., 2010) was adapted to measure the temporal resolution of the mouse vision under scotopic conditions. In brief, mice were trained to associate sinusoidal variations in intensity about a mean level (flicker) with the availability of water at a lick spout during their innate wheel-running behavior (Video 1). Flicker training consisted of computer-triggered modulation of light intensity after a criterion number of wheel revolutions, with flicker frequency, Michelson contrast (referred to hereafter as contrast), and mean intensity varying over subsequent nights of training. Data acquisition began once the mouse could successfully detect flicker across multiple frequencies, contrast levels, and intensities. Each mouse completed ~50 trials each night.

Frequency of seeing curves (percent success vs. contrast) was fit with a Hill function and thresholds defined

Table 1. Parameters describing the rod dim flash response in vivo

Parameter	Description	Value	
		Ex vivo ^a	In vivo
k_R^*	Rate of R^* deactivation (s^{-1})	25	—
k_E	Rate of G^*E^* deactivation (s^{-1})	5 (WT) or 12.5 (RGS9-ox)	8 (WT) or 21.7 (RGS9-ox)
ν_{RE}	Max rate of G^*E^* activation per R^* (s^{-1})	300	350
β_{idv}^b	Rate of cGMP hydrolysis per G^*E^* (s^{-1})	43	—
β_{dark}	Rate of spontaneous cGMP hydrolysis (s^{-1})	4.1	—
D_{cG}^b	Longitudinal diffusion coefficient of cGMP ($\mu m^2 s^{-1}$)	40	—
f_{Ca}^b	Fraction of current carried by calcium	0.12	—
α_{dark}^c	Dark cGMP synthesis rate ($\mu M s^{-1}$)	16.7	19.1
Ca_{dark}^b	Dark adapted Ca^{2+} concentration (nM)	320	Set by α_{dark}
cG_{dark}^b	Dark adapted cGMP concentration (μM)	4.1	Set by α_{dark} and β_{dark}
B_{Ca}^b	Calcium buffer capacity	50	—
n_{cyc}^b	Hill coefficient for Ca^{2+} dependence of cGMP synthesis	1.5	—
K_{cyc}^b	$K_{1/2}$ for Ca^{2+} dependence of cGMP synthesis (nM)	80	—
α_{max}	Max rate of cGMP synthesis ($\mu M s^{-1}$)	150	172
K_{ex}	$K_{1/2}$ for NCKX activation (μM)	1.1	—
J_{ex}^{sat}	Maximum NCKX current ($pA \mu m^{-1}$)	0.21	—

^aGross et al. (2012a).^bValue was held fixed for all simulations.^cValue was adjusted so that for both ex vivo and in vivo, $\alpha_{dark}/\alpha_{max} = 9$.

as the contrast at which the mouse successfully obtained water in 50% of trials. Contrast sensitivities were obtained by taking the inverse of these modulation thresholds, and the logarithm of contrast sensitivities was plotted as a function of stimulus frequency.

Light intensities were measured with a calibrated photodiode and converted into photoisomerizations per rod (R^*) using the following equation (Naarendorp et al., 2010):

$$R^* = F_{cornea} \frac{A_{pupil}}{A_{retina}} T_{media} a_c$$

where F_{cornea} is the flux of photons at the corneal surface (photon density measured with the photodiode); A_{pupil} is the effective area of the undilated mouse pupil, 2 mm² (Naarendorp et al., 2010); A_{retina} is the area of the retina subtended by the stimulus (0.0191 mm²); T_{media} is the transmission of the ocular media, which we assumed to be unity; and a_c is the end-on collecting area.

Modeling

A spatiotemporal model of rod phototransduction (Gross et al., 2012b) was applied to the in vivo WT and GCAPs^{-/-} dim flash responses using the parameter values shown in Table 1. Both WT and GCAPs^{-/-} responses were fit simultaneously by minimizing the normalized and summed mean squared error and assuming the test flash produced three R^* evenly spaced along the longitudinal axis of the outer segment (OS).

Online supplemental material

Fig. S1 illustrates the origin of field potential generating the a -wave component of the ERG and its relevance to the paired flash paradigm, which is described in the

Appendix. Video 1 illustrates the behavioral paradigm used to evaluate temporal contrast sensitivity in Fig. 4.

RESULTS

Isolation of the rod response in the living animal by means of the paired flash ERG paradigm

The flash-activated ERG is a composite, trans-retinal field potential generated by extracellular currents of polarized retinal neurons whose ion channel distributions create radial current dipoles. ERG recordings in vivo are made possible by the electrical separation of the posterior neural retina from the highly conductive underlying vascular tissue of the choroid by the low conductivity pigment epithelium layer. In contrast, the anterior retinal surface abuts the highly conductive, intraocular media, allowing the trans-retinal ERG to be readily recorded as the potential difference between a corneal electrode and a suitably placed reference electrode. The most prominent and mechanistically understood components of the ERG are the a -wave and b -wave. The a -wave, the initial, negative-going component of the ERG (Fig. 1 A and Fig. S1 D), is driven by the suppression of the circulating dark current of photoreceptors (Hagins et al., 1970; Hood and Birch, 1993), whereas the b -wave is predominantly produced by depolarizing bipolar cells and other neurons (for review see Pugh et al., 1998).

The ERG a -wave provides a means of measuring rod photoresponses in vivo (Hood and Birch, 1993; Pugh and Lamb, 1993), though isolating the photoreceptor-driven component from the composite response requires consideration of the b -wave, whose intrusion sums with and distorts the a -wave in a time- and light

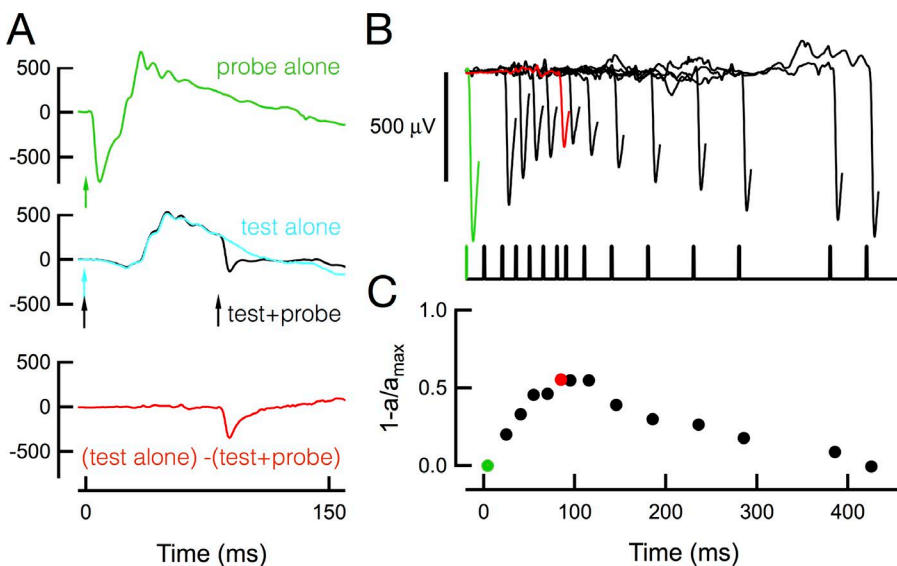


Figure 1. The paired flash protocol unmasks the time course of the rod response in vivo. (A) A bright probe flash ($7.6 \times 10^5 R^*/\text{rod}$) elicited a maximal ERG response (green trace) with a large negative-going *a*-wave, whereas a dim test flash ($284 R^*/\text{rod}$, cyan) elicited a response (cyan trace) with a small *a*-wave component. When the probe flash was presented 80 ms after the dim test flash (black arrows), the response to the probe flash was greatly reduced (black trace) relative to its amplitude in the dark-adapted state (green trace). The cyan trace was subtracted from the black trace to isolate the pure probe response at a delay of 80 ms (red trace). (B) Pairing the bright probe and dim test flashes at delay intervals *t* yielded probe responses that varied in amplitude over time (top traces; bottom trace is a flash monitor for the probe flash). (C) Symbols plot the complement

of the amplitude of the probe *a*-wave responses normalized by the maximum probe flash amplitude (a_{max} , from green trace) as a function of the time interval between the test and probe flashes. All traces were from individual trials of the same animal in the same recording session. The green and red traces in A and B are the same, and the colored symbols in C plot the corresponding photoresponse amplitudes.

intensity-dependent manner (Fig. S1 D). The paired flash paradigm developed by Birch et al. (1995) overcomes this complication, and has been used to extract the time course of murine rod photoresponses (Lyubarsky and Pugh, 1996; Hetling and Pepperberg, 1999). In the paired flash paradigm, a less intense “test” flash that may only partially suppress the photoreceptor dark current is paired at prescribed times with a subsequent, much more intense probe flash that completely suppresses the dark current (Fig. 1 A). By comparing the amplitude of the *a*-wave response to the probe delivered at various delays after the test flash to that of the response to the probe alone, the time course of the underlying rod photoresponse can be derived. Recent work has shown that ERG response to a single flash includes a capacitive component that accounts for up to 60% of the *a*-wave amplitude (Robson and Frishman, 2014). This capacitive component does not affect the recovery of the underlying photoresponse time course with the paired flash paradigm, because the ratio of the capacitive and photocurrent components to the fixed-intensity probe should be constant during the response to the test (see Appendix). In our experiments, the *a*-wave response to the probe flash delivered at various times after the test flash was isolated by subtraction of the response to the test alone from the response to the test plus probe combination (Fig. 1, A and B). The normalized photoresponse to the test flash was then determined for each time point *t* in the series as

$$\frac{r(t, R^*)}{r_{\text{max}}} = 1 - \frac{a(t, R^*)}{a_{\text{max}}}.$$

Here, R^* is the test flash intensity in photoisomerizations/rod, $a(t, R^*)$ is the amplitude of the *a*-wave response to the probe delivered at time *t* after the test, and a_{max} is the amplitude of the *a*-wave response to the probe in the dark-adapted eye. The application of this analysis for a test flash that produced $280 R^*$ yielded a fractional photocurrent suppression that peaked at ~ 100 ms and reached an amplitude of $\sim 60\%$ the maximum (Fig. 1, B and C; also see Appendix).

The rod response has faster time course in vivo than ex vivo

We repeated the paired flash paradigm with test flashes of varied strength to generate an entire family of responses of rods in vivo (Fig. 2 A). As the strength of the test flash increased, the amplitude also increased until a saturated level was reached. The resulting response family was qualitatively similar to rod response families measured ex vivo with suction electrodes (Fig. 2 B). Quantitatively, however, the in vivo responses exhibited a faster time to peak (~ 90 ms vs. ~ 125 ms) and returned to baseline more rapidly than the ex vivo responses at comparable levels of fractional dark current suppression (Fig. 2, A and B). Both in vivo and ex vivo response-intensity relations were well described by exponential saturation functions, though that for the in vivo experiments was shifted to higher light levels (Fig. 2 C).

One mechanism that potentially constrains the amplitude of the rod single photon response in ex vivo recordings is calcium feedback regulation of guanylate cyclase (Burns et al., 2002; Gross et al., 2012a). In normal rods, delayed activation of guanylate cyclase by

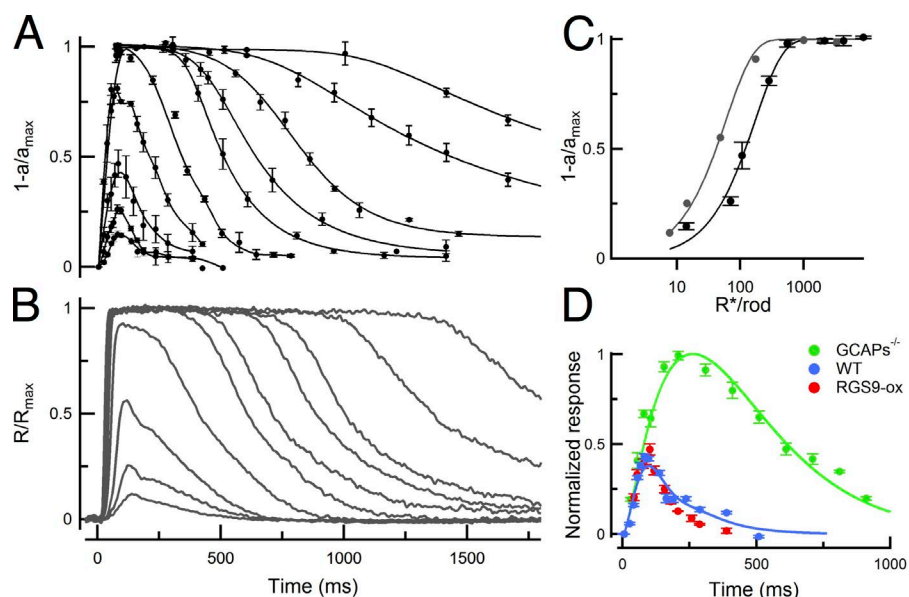


Figure 2. Molecular underpinnings of rod in vivo kinetics. (A) Normalized population average in vivo flash family obtained via the paired flash protocol in response to test flashes calculated to produce 14, 70, 107, 285, 550, 2,150, 4,280, 8,770, 17,500, and 35,100 R^*/rod . Symbols plot the mean \pm SEM ($n = 3-6$ mice) and are connected by cubic splines. (B) Representative family of responses obtained from an intact rod using suction electrode recording in response to flashes producing 7, 14, 48, 174, 585, 997, 1,870, 3,300, 6,330, 13,400, and 25,100 R^*/rod . (C) Response amplitudes plotted as a function of test flash strength for the data obtained in vivo (A, black) and ex vivo (B, gray); smooth curves are exponential saturation functions. (D) Dim flash responses from WT ($n = 6$), RGS9-ox ($n = 4$), and GCAPs $^{-/-}$ ($n = 4$) mice, fitted by the phototransduction spatiotemporal model of Gross et al. (2012a) with parameters given in Table 1. All traces represent the response to a flash of the same light intensity and are normalized by the peak amplitude of the GCAPs $^{-/-}$ response. The blue symbols present a normalized version of the response to the dimmest flash in A. Error bars represent SEM.

GCAPs causes subsaturating flash responses to show a characteristic accelerated recovery or “nose” after reaching peak amplitude. Both ex vivo and in vivo flash responses showed this characteristic kinetic feature for intermediate flash strengths, implicating strong calcium feedback regulation in both recording conditions. To determine the extent to which calcium feedback to cGMP synthesis affected the dim flash response in vivo, we used the paired flash paradigm to extract the time course of the rod dim flash response of GCAPs $^{-/-}$ mice (Mendez et al., 2001). The dim flash response of GCAPs $^{-/-}$ mice rose on a common initial trajectory, but for a longer time, reaching a much larger peak amplitude and recovering more slowly than the WT response (Fig. 2 D). The changes in response amplitude and kinetics with GCAPs deletion are similar to those previously measured in ex vivo recordings (Mendez et al., 2001; Burns et al., 2002; Okawa et al., 2010; Gross et al., 2012a). This suggested that application of the spatiotemporal model of the phototransduction cascade previously shown to describe single-photon responses of both WT and GCAPs $^{-/-}$ rods to the ex vivo dim flash responses (Gross et al., 2012b) could provide insight into the mechanisms responsible for the relatively faster in vivo rod response kinetics (Fig. 2 D, curves). Good agreement between the model and the in vivo data were obtained with kinetic parameters (Table 1) similar to those used to predict single-photon responses of rods of

both genotypes recorded ex vivo (Gross et al., 2012a). A notable exception was that the deactivation rate constant of the G-protein–phosphodiesterase (PDE) complex in vivo was estimated to be 8 s^{-1} , substantially faster than the rate 5 s^{-1} rate constant established to be the rate-limiting step governing rod response deactivation in ex vivo recordings. Thus, the theoretical analysis supports the hypothesis that the rate of G-protein PDE deactivation is considerably faster in vivo than ex vivo.

To test whether RGS9-mediated deactivation of the G-protein–PDE complex governs dim flash response recovery in vivo, we used the paired flash method to measure the dim flash response of RGS9-overexpressing mice (RGS9-ox; Fig. 2 D, red symbols). Unlike dim flash responses obtained in ex vivo recordings (Krispel et al., 2006; Gross and Burns, 2010), those of RGS9-ox and WT extracted from in vivo paired flash data were very similar, though the final recovery phase of the RGS9-ox response was only slightly but reliably faster than that of WT mice. The overall similarity of the dim flash responses could arise either because RGS9-catalyzed GTPase is not rate-limiting for recovery in vivo or because strong calcium feedback to cGMP synthesis is insufficiently fast enough in vivo to “follow” the faster underlying PDE deactivation (Gross et al., 2012a). Because bright flashes that saturate the rods drive calcium to a constant low level, responses to such flashes can be used to measure the kinetics of the transduction deacti-

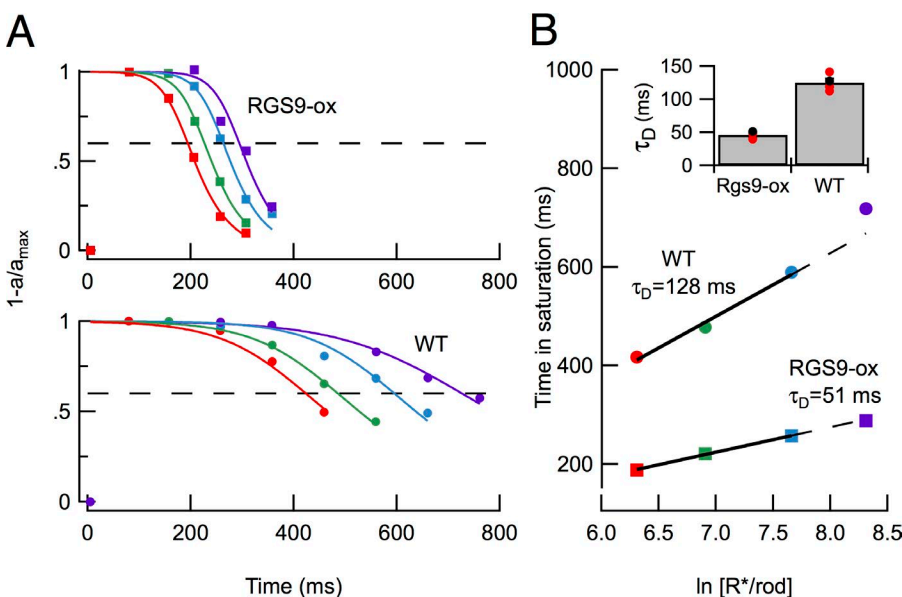


Figure 3. Rod recovery from bright flashes is rate limited by RGS9 expression in vivo. (A) Photoresponse recovery from saturating flashes of increasing strength from an RGS9-ox mouse (top, squares) and a WT mouse (bottom, circles). Colors denote the flash strengths corresponding to the points in B. Note that the timescale of the bottom panel is twofold longer than that of the top panel. (B) Times for the photoresponses in A to recover to 60% of their dark-adapted value (dashed lines in A) as a function of the natural logarithm of the number of photoexcited rhodopsin molecules (R^*/rod) elicited by the test flash. When there is translation invariance in the recovery of responses (Nikonov et al., 1998), the slope of the fitted line gives the dominant time constant of recovery (τ_D). (inset) Individual τ_D determinations (red points) and means (given by the height of the bars) for the two different genetic backgrounds ($n = 3$ mice each). Black points in the inset correspond to the values obtained from the data in A and B.

vation step without the effects of calcium feedback mechanisms (Pepperberg et al., 1992; Lyubarsky and Pugh, 1996). Thus, we proceeded to use saturating flash responses to measure the dominant, rate-limiting step for photoresponse recovery in vivo.

G-protein deactivation rate-limits the dominant recovery time constant in vivo

To measure the dominant time constant of recovery, we used the paired flash method to extract the recoveries of rod responses to saturating probe flashes from both WT and RGS9-ox mice (Fig. 3, A and B). In each experiment, the recovery time course to flashes of at least four different flash strengths were measured. The recovery time courses of each mouse strain showed approximate translation invariance for the three lower saturating flash intensities (Fig. 3 A, red, green, and blue), whereas further increases of the flash strength caused the WT recovery to follow a somewhat slower trajectory (Fig. 3 A, purple). The times needed for the in vivo rod responses to recover to 60% of its maximal value (Fig. 3 A, dashed lines) were measured and plotted against the natural logarithm of the test flash strength (Fig. 3 B); this analysis yields a line whose slope reflects the dominant time constant (τ_D) of recovery (Pepperberg et al., 1992; Lyubarsky and Pugh, 1996). In a population of WT mice, the mean τ_D was 125 ± 12 ms (mean \pm SEM, $n = 3$), consistent with the mean lifetime of the G-protein–PDE complex used in fitting the dim flash response (Fig. 2 D; $1/8 \text{ s}^{-1} = 125 \text{ ms}$) but nearly half that previously determined from recording of WT rods ex vivo (Krispel et al., 2006; Gross and Burns, 2010). Surprisingly, the value of

τ_D for RGS9-ox animals was nearly three times shorter than that for WT mice (Fig. 3 B; $P = 0.0002$). Together, these results show that rod recovery kinetics are much faster in vivo than ex vivo and that the deactivation of the G-protein–effector complex catalyzed by the RGS9 complex is normally the rate-limiting step for recovery from bright flashes in vivo.

Behavioral measures of the temporal acuity of rod-mediated vision

Rods that overexpress the RGS9 complex show markedly faster recovery kinetics from both dim and bright flashes ex vivo (Krispel et al., 2006), and multiple classes of retinal bipolar cells downstream of these accelerated rods show greater amplitude flicker modulation under scotopic conditions ex vivo (Fortenbach et al., 2015). Thus, we predicted that RGS9-ox mice should behaviorally demonstrate higher scotopic temporal contrast sensitivity than WT animals at high flicker frequencies. To test this prediction, we measured temporal contrast sensitivity of both WT and RGS9-ox mice using the nocturnal wheel-running assay previously used to measure mouse visual thresholds (Naarendorp et al., 2010; Fig. 4, A and B). Mice were trained to associate the flickering of the light intensity of a small (5 deg) target with the availability of water from a spout; computer-controlled random variations in contrast for different mean intensities and flicker frequencies were used to measure the temporal contrast sensitivity of scotopic vision (Fig. 4). The mice became more successful at correctly detecting the flicker as the contrast increased (Fig. 4 C); a plot of the contrast threshold as a function of flicker

frequency yielded contrast sensitivity functions (CSFs; Fig. 4, D–F) similar in form to those previously reported for individual mouse retinal neurons (Burkhardt et al., 2007), mouse behavioral experiments (Umino et al., 2008) and human psychophysical studies (Kelly, 1961). In dim ambient light that generated, on average, 50 $R^*/\text{rod/s}$, WT mice readily detected flicker at 10 Hz (Fig. 4 D, black), a frequency that rods *ex vivo* could not follow (Fortenbach et al., 2015). Surprisingly, RGS9-ox mice showed similar contrast sensitivity at low flicker frequencies and markedly poorer performance at 10 Hz than WT mice (Fig. 4 D). Because RGS9 overexpression reduces the steady-state light-driven PDE activity of the rods roughly twofold (Fortenbach et al., 2015), we also compared the CSFs of WT and RGS9-ox mice obtained at twofold different intensities and thus producing equivalent levels of steady-state light activation. Comparing WT and RGS9-ox mice with equivalent levels of light-driven PDE activity (Fig. 4 E, 20 and 50 $R^*/\text{rod/s}$; and Fig. 4 F, 50 and 100 $R^*/\text{rod/s}$) revealed that the CSF of RGS9-ox mice consistently had a slightly narrower low-pass bandwidth and failed to show the increase in contrast sensitivity at ~5–8 Hz recently observed in RGS9-ox bipolar cell recordings from retinal slices (Fortenbach et al., 2015). In all cases, RGS9-ox mice showed markedly poorer performance at 10 Hz than WT mice. Thus, although RGS9 overexpression speeds rod recovery *in vivo*, it does not improve the temporal resolution of scotopic vision.

DISCUSSION

The sensitivity and kinetics of rod photoreceptors have driven interpretation of scotopic visual thresholds and contrast response functions for decades (Conner, 1982; Baylor et al., 1984; Hess and Nordby, 1986; Makous, 2004). For such comparisons to be meaningful, the sensitivity and kinetics measured *ex vivo* must adequately reflect rod function *in vivo*. Our experiments have revealed that the kinetics of rod response recovery *in vivo* are about twofold faster than those measured in all previous *ex vivo* experiments. Notably, the same biochemical reaction (RGS9-catalyzed deactivation of the G-protein–PDE complex) is clearly rate limiting for recovery of bright flash responses both *in vivo* (Fig. 3) and *ex vivo* (Krispel et al., 2006). In the living animal, overexpression of RGS9 accelerated τ_D from the normal value of 128 ms (WT) to 51 ms (RGS9-ox), a 2.5-fold change. In suction electrode recordings made from rods of the same mouse strains, τ_D decreased from 250 ms to 75 ms with RGS9-ox (Krispel et al., 2006), a 3.3-fold change. Thus, RGS9 overexpression has a qualitatively similar effect on response recovery *in vivo* and *ex vivo*, though all *in vivo* responses were faster.

For responses to dim flashes, RGS9 overexpression likewise led to faster recovery, but the effect was much

less dramatic *in vivo* (Fig. 2). It is difficult to interpret the small difference between WT and RGS9-ox dim flash responses because at late times (200–500 ms), the signals being measured with the paired flash method are very small. Nevertheless, we note that for the single exponential decay of G-protein–PDE activity to dominate response recovery, its time constant must be sufficiently longer than other deactivation steps (like rhodopsin shutoff), and calcium feedback equilibration must be fast relative to cascade deactivation steps (Nikonov et al., 1998). Thus, if G-protein deactivation in RGS9-ox mice proceeds with a time constant of 51 ms for dim flashes (as it does for bright flashes; Fig. 3 B), it would be expected to substantially overlap with the 40-ms time constant for rhodopsin deactivation (Gross and Burns, 2010), resulting in a recovery time course limited by the convolved effect of the two deactivation mechanisms.

Rod phototransduction kinetics *in vivo*: implications for rod signaling

For decades, the most common method for studying light responses of rod photoreceptors has been suction electrode recordings from the OSs of intact cells (Baylor et al., 1979). This technique is greatly preferable to whole-cell recording for measuring phototransduction kinetics because recordings from intact rods obviate the diffusional loss of soluble proteins and spatial disruption of metabolites and second messengers essential for normal enzymatic activities and channel conductances. However, both suction electrode and whole-cell recording methods require removal of the retina, as well as slicing and bath perfusion of a physiological saline. In the intact eye, the subretinal space that surrounds the OSs is bounded by structures that create a unique extracellular milieu: on one side, the endfeet of Müller glial cells are adjoined by adherens junctions, forming what is known as the external limiting membrane; and on the other side, the retinal pigment epithelial cells are conjoined by tight junctions, forming the blood–retinal barrier between choroidal vasculature and retina. Indeed, previous studies have shown that in some targeted mutant mice, *in vivo* ERG recordings suggest highly dysfunctional photoreceptors, whereas *ex vivo* recordings are nearly normal (Jiang et al., 1996; Daniele et al., 2008; Sherry et al., 2010), underscoring the importance of regulation of the subretinal milieu and revealing limitations of *ex vivo* recordings for understanding disease processes that alter this milieu.

However, there is more to the story than simply whether or not these boundaries confining the subretinal environment are breeched. It has also long been known that recording from photoreceptors in different physiological saline solutions produces responses with considerably different amplitudes and kinetics. For example, bathing solutions with HEPES-

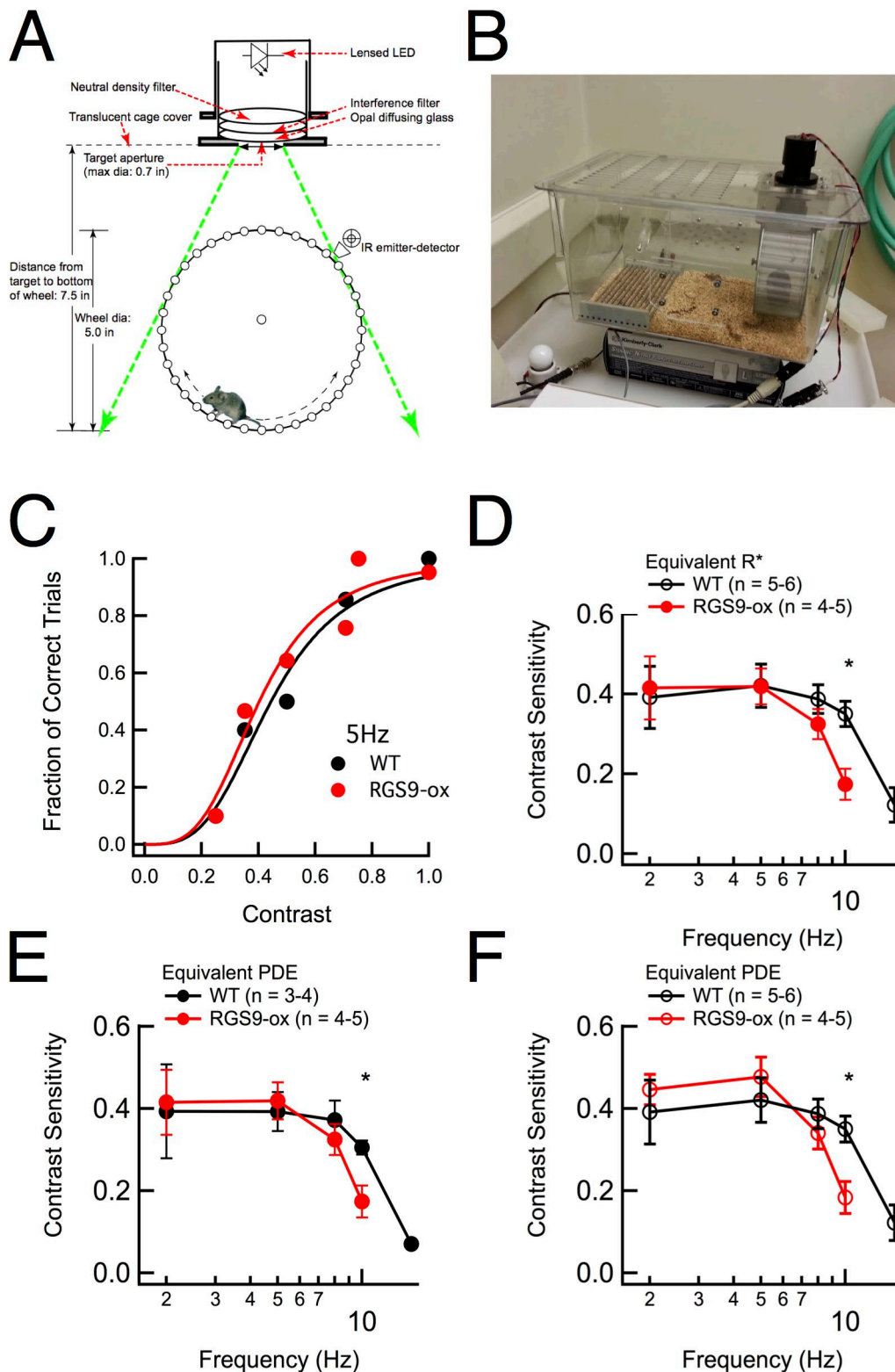


Figure 4. **RGS9 overexpression in rods does not improve temporal contrast sensitivity.** (A) Schematic details of the custom wheel-running visual behavioral apparatus, reprinted with permission from Naarendorp et al. (2010). (B) Photograph of the behavioral apparatus, with the mouse on the running wheel with the LED delivering the green flickering light mounted above. Flicker detection was measured by the trained mouse exiting the wheel and licking the water spout mounted above the elevated steel wire floor (left side of cage), completing a circuit and creating a TTL pulse recorded by the computer. Actual trials were performed in a completely dark room, and the cage was surrounded by an opaque-white ventilated enclosure illuminated from within by adjustable intensity white lights (bottom left of the picture), mounted below the floor level of the cage to avoid direct illumination. (C) Repre-

based pH buffers produce responses that are much slower than those measured in solutions buffered with bicarbonate (Lamb et al., 1981). In addition, two different bicarbonate-based buffers, Ames' media and Locke's solution, lead to rod photoresponses with very different time courses, with Locke's solution producing markedly smaller and faster single-photon responses (Gross and Burns, 2010; Azevedo and Rieke, 2011) but higher than normal spontaneous spiking from inner retinal neurons (Azevedo and Rieke, 2011). Here, we have shown that rod responses in vivo are even faster than the fastest suction electrode recordings reported (in Locke's). These new results unequivocally show that the large, slow rod responses characteristic of Ames' solutions are clearly less representative of rod behavior in vivo, an important consideration going forward because Ames' is currently considered the gold-standard recording medium for virtually every laboratory recording from retinal slices. Thus, inferences about the processing of single-photon responses through the retinal circuitry ex vivo may be incorrect.

It is also important to note that the paired flash paradigm has been previously used to determine the dominant time constant of rod photocurrent recovery from bright flashes in mice and found to be considerably slower than that measured here (210 ms [Lyubarsky and Pugh, 1996] vs. 125 ms [Fig. 2]). Possible explanations include a difference in mouse strains (CBA/CAJ vs. C57BL/6J) and a difference in the anesthesia protocols, which could also cause differences in ocular temperature. For example, Lyubarsky and Pugh (1996) used relatively heavy sedation with ketamine-xylazine, whereas this study used isoflurane, from which animals recovered very rapidly (<5 min) upon anesthetic removal. Recent studies have demonstrated that ketamine rapidly increases phosphorylation of many targets and activation of several ubiquitous kinases like mTOR, p70S6 kinase, and ERK (reviewed in Duman et al., 2012). Because phosphorylation of RGS9 has been associated with reduced GTPase activity (Balasubramanian et al., 2001; Sokal et al., 2003), it is possible that ketamine could also slow rod photoreceptor recovery by promoting phosphorylation of RGS9. Were an effect of different anesthetics on RGS9-catalyzed deactivation to be confirmed, it might lead to testable hypotheses that could explain the differences between in vivo and ex vivo recordings.

Implications for vision

Single-photon detection requires that rods generate sizable responses from single photoexcited rhodopsins. The transmission of single-photon responses from rods to rod bipolar cells depends on the amplitude of these responses rather than the overall time course of the unitary event (Field and Rieke, 2002; Okawa et al., 2010). As a result, RGS9-ox mice under single-photon conditions show no change in temporal contrast sensitivity measured with optomotor responses (Umino et al., 2012).

In the presence of higher light intensities that produce more than one photoexcited rhodopsin per response integration time, the time course of the rod unitary response can impact temporal resolution of vision. This is true both at the single photoreceptor level (Gross et al., 2012a; Arshavsky and Burns, 2014) and the level of rod bipolar cells in retinal slices (Field and Rieke, 2002; Fortenbach et al., 2015). When the RGS9 complex is overexpressed in rods (RGS9-ox), rods display greater amplitude current fluctuations in response to flicker (1–8 Hz) but roughly twofold lower sensitivity, owing to the faster than normal G-protein deactivation and thus lower steady-state levels of PDE activation (Fortenbach et al., 2015). Recordings from both ON and OFF bipolar cells downstream of these faster, less sensitive RGS9-ox rods likewise show greater amplitude current and voltage modulation in response to scotopic flicker (5–8 Hz), indicating that the synaptic transfer function is limited under scotopic conditions by the sluggish time course of rod photoreceptor deactivation rather than by rod-bipolar synaptic properties or by intrinsic membrane properties of the cells themselves (Fortenbach et al., 2015). Thus, we expected that RGS9-ox mice would exhibit greater contrast sensitivity than WT mice on the nocturnal wheel-running assay, resulting in a significant vertical upward shift over the range of at least 5–8 Hz. Instead, the shape of the CSF showed a lower cutoff frequency than that of WT mice, with remarkably poorer performance than normal at 10 Hz (Fig. 4). Given that our results also show that the rod response in vivo is indeed accelerated by RGS9 overexpression (Fig. 3 A) and that in vivo *b*-wave scotopic flicker responses and ex vivo bipolar responses are likewise enhanced in RGS9-ox mice (Fortenbach et al., 2015), we conclude that a phenomenon or process downstream of the retinal bipolar cells serves as a kinetic bottleneck preventing the use of this higher frequency visual information under scotopic conditions. It

sentative frequency of seeing curves for an RGS9-ox transgenic mouse and a WT littermate performing the nocturnal wheel-running assay for flicker detection. (D–F) Contrast sensitivity (inverse of the contrast producing 50% correct trials) for both strains was similar, though RGS9-ox mice showed more narrow frequency tuning, reflecting impaired visual performance at higher frequencies. The impairment at 10 Hz was significant (*, $P < 0.05$) regardless of whether data from the same absolute stimulus intensity were compared (D; 50 R^* /rod/s) or whether the light intensities were adjusted to produce equivalent PDE activation (E and F), owing to the faster deactivation of the transducin–PDE complex in the RGS9-ox mice (Fortenbach et al., 2015). (E) 23 and 50 R^* /rod/s for WT and RGS9-ox mice, respectively. (F) 50 and 104 R^* /rod/s for WT and RGS9-ox mice, respectively. Error bars represent SEM.

is possible that differentially altering the ON and OFF bipolar cell temporal properties (via RGS9-ox; Fortenbach et al., 2015) disrupts convergent coordination downstream, similar to destructive interference between “slow” and “fast” rod signals described in human psychophysics (e.g., Conner, 1982). Thus, it may be that downstream pathways are adapted to maximize information from upstream inputs that are shaped by regulators like RGS9 and that a kinetic bottleneck is artificially produced when rod responses are accelerated by RGS9 overexpression. Future work is needed to test this idea and determine the mechanism limiting rod signals in the inner retina and beyond.

APPENDIX

In the dark-adapted eye, retinal photoreceptors have inward membrane current in the OS layer through CNG channels and balancing outward membrane current in the rest of the photoreceptor layer through K^+ -selective channels (Fig. S1 A). The spatial separation of the inward and outward membrane currents produces a “circulating” current, whose radial extracellular limb generates a trans-retinal field potential that makes the vitreal side of the retina positive with respect to the tips of the OSs (Hagins et al., 1970). The ERG *a*-wave has long been understood as arising primarily from light suppression of the rod circulating current and the corresponding decline of its field potential. Recent analysis by Robson and Frishman (2014), however, has revealed that a major component of the *a*-wave arises from a field potential generated by the extracellular flow of capacitive current triggered by rapid closure of the CNG channels. The purpose of this appendix is to explain why the paired flash *a*-wave method developed by Lyubarsky and Pugh (1996) and applied here to extract the time course of the rod photoreponse remains valid within the framework of the Robson–Frishman analysis. (For the section that follows, the reader should refer to the paired flash protocol of Fig. 1, keeping in mind the distinction between the “test” flash, which may only partially suppress the circulating current, and the “probe” flash, an intense flash that rapidly and completely suppresses all residual circulating current, and that is delivered at various times after the test flash.)

Consider first the response to the probe flash delivered to the dark-adapted retina. For such a flash, the *a*-wave amplitude is proportional to the maximum rod CNG current and the resultant capacitive current:

$$a_{\max} = k_1 J_{cG,\max} + k_2 J_{c,\max}. \quad (\text{A1})$$

In Eq. A1, $J_{cG,\max}$ represents the maximum whole-cell CNG current and $J_{c,\max}$ the amplitude of the correspond-

ing capacitive transient resulting from rapid suppression of the CNG current. Considering the rod as a whole-cell circuit, $J_{c,\max}$ is negatively proportional to $J_{cG,\max}$ (e.g., Cobbs and Pugh, 1987). However, because the *a*-wave is a field potential arising from extracellular currents (Fig. S1), the signs and magnitudes of the proportionality constants k_1 and k_2 depend on the rod density and on the radial distribution of the circulating and capacitive currents, respectively, and on the extracellular and intracellular resistance profiles (Hagins et al., 1970; Robson and Frishman, 2014). The value of $J_{c,\max}$ also depends on the probe flash intensity, which determines how rapidly the CNG channels close and the membrane hyperpolarizes. Based on the analysis of Robson and Frishman (2014) and on our own analysis, for the probe flash used in our experiments the fraction of a_{\max} arising from the suppression of the CNG current is $\sim 50\%$.

Next, consider the *a*-wave responses to the probe flash delivered at various times t after the presentation of a test flash that produces R^* isomerizations/rod (compare with Fig. 1). In this case, the amplitude of the *a*-wave response to the probe recorded at time t is expressible as

$$a(t, R^*) = k_1 J_{cG}(t, R^*) + k_2 J_c(t, R^*). \quad (\text{A2})$$

In Eq. A2, $J_{cG}(t, R^*)$ is the residual CNG current present at the moment of the probe flash, and $J_c(t, R^*)$ is the corresponding capacitive current generated as the probe completely suppresses J_{cG} . For the fixed-intensity probe flash, the ratio of the contributions of the capacitive current and the CNG current suppression to the *a*-wave will be constant:

$$\rho = k_2 J_c(t, R^*) / k_1 J_{cG}(t, R^*) \approx \text{const.} \quad (\text{A3})$$

This follows, because $J_c(t, R^*)$ is proportional to $J_{cG}(t, R^*)$, and the cellular and spatial factors that determine to the values of k_1 and k_2 can be considered invariant during the response to the test flash. By taking the ratio of Eq. A2 to Eq. A1 and substituting from Eq. A3, one finds

$$\frac{J_{cG}(t, R^*)}{J_{cG,\max}} = \frac{a(t, R^*)}{a_{\max}}.$$

Thus, the normalized photocurrent response (the time course of CNG current suppression by the test flash) is given by

$$\frac{r(t, R^*)}{r_{\max}} \equiv 1 - \frac{J_{cG}(t, R^*)}{J_{cG,\max}} = 1 - \frac{a(t, R^*)}{a_{\max}}, \quad (\text{A4})$$

where “ \equiv ” signifies a definition. Accordingly, we applied Eq. A4 to recover the time course of in vivo rod photoreponses to test flashes from the probe flash *a*-wave amplitudes (Fig. 1).

ACKNOWLEDGMENTS

This work was supported by the National Eye Institute (NEI) grants R01-EY14047 and R01-EY02660, the University of California, Davis (UC Davis), NEI vision core grant P30-EY012576, and UC Davis NEI vision training grant T32-EY015387.

The authors declare no competing financial interests.

Author contributions: G. Peinado Allina performed the ERG experimental design and execution, assembled the figures, and drafted the manuscript; C. Fortenbach performed the behavioral experiments and analyzed the data; O.P. Gross performed the modeling; F. Naarendorp designed the behavioral apparatuses and training protocol for the flicker stimuli and assisted in setting up the behavioral experiments at UC Davis; E.N. Pugh Jr. participated in experimental design and directed data analysis; and M.E. Burns directed experimental design and interpretation and wrote the manuscript. All authors edited the manuscript.

Angus C. Nairn served as editor.

Submitted: 9 September 2016

Accepted: 8 February 2017

REFERENCES

- Arshavsky, V.Y., and M.E. Burns. 2014. Current understanding of signal amplification in phototransduction. *Cell. Logist.* 4:e29390. <http://dx.doi.org/10.4161/cl.29390>
- Azevedo, A.W., and F. Rieke. 2011. Experimental protocols alter phototransduction: The implications for retinal processing at visual threshold. *J. Neurosci.* 31:3670–3682. <http://dx.doi.org/10.1523/JNEUROSCI.4750-10.2011>
- Balasubramanian, N., K. Levay, T. Keren-Raifman, E. Faurobert, and V.Z. Slepak. 2001. Phosphorylation of the regulator of G protein signaling RGS9-1 by protein kinase A is a potential mechanism of light- and Ca²⁺-mediated regulation of G protein function in photoreceptors. *Biochemistry.* 40:12619–12627. <http://dx.doi.org/10.1021/bi015624b>
- Baylor, D.A., T.D. Lamb, and K.W. Yau. 1979. The membrane current of single rod outer segments. *J. Physiol.* 288:589–611.
- Baylor, D.A., B.J. Nunn, and J.L. Schnapf. 1984. The photocurrent, noise and spectral sensitivity of rods of the monkey *Macaca fascicularis*. *J. Physiol.* 357:575–607. <http://dx.doi.org/10.1113/jphysiol.1984.sp015518>
- Birch, D.G., D.C. Hood, S. Nusinowitz, and D.R. Pepperberg. 1995. Abnormal activation and inactivation mechanisms of rod transduction in patients with autosomal dominant retinitis pigmentosa and the pro-23-his mutation. *Invest. Ophthalmol. Vis. Sci.* 36:1603–1614.
- Burkhardt, D.A., P.K. Fahey, and M.A. Sikora. 2007. Retinal bipolar cells: temporal filtering of signals from cone photoreceptors. *Vis. Neurosci.* 24:765–774. <http://dx.doi.org/10.1017/S0952523807070630>
- Burns, M.E., A. Mendez, J. Chen, and D.A. Baylor. 2002. Dynamics of cyclic GMP synthesis in retinal rods. *Neuron.* 36:81–91. [http://dx.doi.org/10.1016/S0896-6273\(02\)00911-X](http://dx.doi.org/10.1016/S0896-6273(02)00911-X)
- Cobbs, W.H., and E.N. Pugh Jr. 1987. Kinetics and components of the flash photocurrent of isolated retinal rods of the larval salamander, *Ambystoma tigrinum*. *J. Physiol.* 394:529–572. <http://dx.doi.org/10.1113/jphysiol.1987.sp016884>
- Conner, J.D. 1982. The temporal properties of rod vision. *J. Physiol.* 332:139–155. <http://dx.doi.org/10.1113/jphysiol.1982.sp014406>
- Daniele, L.L., B. Sauer, S.M. Gallagher, E.N. Pugh Jr., and N.J. Philp. 2008. Altered visual function in monocarboxylate transporter 3 (Slc16a8) knockout mice. *Am. J. Physiol. Cell Physiol.* 295:C451–C457. <http://dx.doi.org/10.1152/ajpcell.00124.2008>
- Duman, R.S., N. Li, R.J. Liu, V. Duric, and G. Aghajanian. 2012. Signaling pathways underlying the rapid antidepressant actions of ketamine. *Neuropharmacology.* 62:35–41. <http://dx.doi.org/10.1016/j.neuropharm.2011.08.044>
- Field, G.D., and F. Rieke. 2002. Nonlinear signal transfer from mouse rods to bipolar cells and implications for visual sensitivity. *Neuron.* 34:773–785. [http://dx.doi.org/10.1016/S0896-6273\(02\)00700-6](http://dx.doi.org/10.1016/S0896-6273(02)00700-6)
- Fortenbach, C.R., C. Kessler, G. Peinado Allina, and M.E. Burns. 2015. Speeding rod recovery improves temporal resolution in the retina. *Vision Res.* 110(Pt A):57–67. <http://dx.doi.org/10.1016/j.visres.2015.02.011>
- Gross, O.P., and M.E. Burns. 2010. Control of rhodopsin's active lifetime by arrestin-1 expression in mammalian rods. *J. Neurosci.* 30:3450–3457. <http://dx.doi.org/10.1523/JNEUROSCI.5391-09.2010>
- Gross, O.P., E.N. Pugh Jr., and M.E. Burns. 2012a. Calcium feedback to cGMP synthesis strongly attenuates single-photon responses driven by long rhodopsin lifetimes. *Neuron.* 76:370–382 (published erratum appears in *Neuron* 2013. 78:949). <http://dx.doi.org/10.1016/j.neuron.2012.07.029>
- Gross, O.P., E.N. Pugh Jr., and M.E. Burns. 2012b. Spatiotemporal cGMP dynamics in living mouse rods. *Biophys. J.* 102:1775–1784. <http://dx.doi.org/10.1016/j.bpj.2012.03.035>
- Hagins, W.A., R.D. Penn, and S. Yoshikami. 1970. Dark current and photocurrent in retinal rods. *Biophys. J.* 10:380–412. [http://dx.doi.org/10.1016/S0006-3495\(70\)86308-1](http://dx.doi.org/10.1016/S0006-3495(70)86308-1)
- Hecht, S., S. Shlaer, and M.H. Pirenne. 1942. Energy, quanta, and vision. *J. Gen. Physiol.* 25:819–840. <http://dx.doi.org/10.1085/jgp.25.6.819>
- Hess, R.F., and K. Nordby. 1986. Spatial and temporal limits of vision in the achromat. *J. Physiol.* 371:365–385. <http://dx.doi.org/10.1113/jphysiol.1986.sp015981>
- Hetling, J.R., and D.R. Pepperberg. 1999. Sensitivity and kinetics of mouse rod flash responses determined in vivo from paired-flash electroretinograms. *J. Physiol.* 516:593–609. <http://dx.doi.org/10.1111/j.1469-7793.1999.0593v.x>
- Hood, D.C., and D.G. Birch. 1993. Light adaptation of human rod receptors: the leading edge of the human a-wave and models of rod receptor activity. *Vis. Res.* 33:1605–1618.
- Jiang, H., A. Lyubarsky, R. Dodd, N. Vardi, E. Pugh, D. Baylor, M.I. Simon, and D. Wu. 1996. Phospholipase C beta 4 is involved in modulating the visual response in mice. *Proc. Natl. Acad. Sci. USA.* 93:14598–14601. <http://dx.doi.org/10.1073/pnas.93.25.14598>
- Kelly, D.H. 1961. Visual response to time-dependent stimuli. I. Amplitude sensitivity measurements. *J. Opt. Soc. Am.* 51:422–429. <http://dx.doi.org/10.1364/JOSA.51.000422>
- Krispel, C.M., D. Chen, N. Melling, Y.J. Chen, K.A. Martemyanov, N. Quillinan, V.Y. Arshavsky, T.G. Wensel, C.K. Chen, and M.E. Burns. 2006. RGS expression rate-limits recovery of rod photoresponses. *Neuron.* 51:409–416. <http://dx.doi.org/10.1016/j.neuron.2006.07.010>
- Lamb, T.D., P.A. McNaughton, and K.W. Yau. 1981. Spatial spread of activation and background desensitization in toad rod outer segments. *J. Physiol.* 319:463–496. <http://dx.doi.org/10.1113/jphysiol.1981.sp013921>
- Lyubarsky, A.L., and E.N. Pugh Jr. 1996. Recovery phase of the murine rod photoresponse reconstructed from electroretinographic recordings. *J. Neurosci.* 16:563–571.
- Lyubarsky, A.L., L.L. Daniele, and E.N. Pugh Jr. 2004. From candelas to photoisomerizations in the mouse eye by rhodopsin bleaching in situ and the light-rearing dependence of the major components of the mouse ERG. *Vision Res.* 44:3235–3251. <http://dx.doi.org/10.1016/j.visres.2004.09.019>
- Makous, W. 2004. Scotopic vision. In *The Visual Neurosciences*. L.M. Chalupa and J.S. Werner, editors. MIT Press, Boston. 838–850.
- Mendez, A., M.E. Burns, I. Sokal, A.M. Dizhoor, W. Baehr, K. Palczewski, D.A. Baylor, and J. Chen. 2001. Role of guanylate cyclase-activating proteins (GCAPs) in setting the flash sensitivity

- of rod photoreceptors. *Proc. Natl. Acad. Sci. USA*. 98:9948–9953. <http://dx.doi.org/10.1073/pnas.171308998>
- Naarendorp, F., T.M. Esdaille, S.M. Banden, J. Andrews-Labenski, O.P. Gross, and E.N. Pugh Jr. 2010. Dark light, rod saturation, and the absolute and incremental sensitivity of mouse cone vision. *J. Neurosci.* 30:12495–12507. <http://dx.doi.org/10.1523/JNEUROSCI.2186-10.2010>
- Nikonov, S., N. Engheta, and E.N. Pugh Jr. 1998. Kinetics of recovery of the dark-adapted salamander rod photoresponse. *J. Gen. Physiol.* 111:7–37. <http://dx.doi.org/10.1085/jgp.111.1.7>
- Nishiguchi, K.M., I. Sokal, L. Yang, N. Roychowdhury, K. Palczewski, E.L. Berson, T.P. Dryja, and W. Baehr. 2004. A novel mutation (I143N) in guanylate cyclase-activating protein 1 (GCAP1) associated with autosomal dominant cone degeneration. *Invest. Ophthalmol. Vis. Sci.* 45:3863–3870. <http://dx.doi.org/10.1167/iops.04-0590>
- Okawa, H., K.J. Miyagishima, A.C. Arman, J.B. Hurley, G.D. Field, and A.P. Sampath. 2010. Optimal processing of photoreceptor signals is required to maximize behavioural sensitivity. *J. Physiol.* 588:1947–1960. <http://dx.doi.org/10.1113/jphysiol.2010.188573>
- Pepperberg, D.R., M.C. Cornwall, M. Kahlert, K.P. Hofmann, J. Jin, G.J. Jones, and H. Ripps. 1992. Light-dependent delay in the falling phase of the retinal rod photoresponse. *Vis. Neurosci.* 8:9–18. <http://dx.doi.org/10.1017/S0952523800006441>
- Pepperberg, D.R., D.G. Birch, and D.C. Hood. 1997. Photoresponses of human rods in vivo derived from paired-flash electroretinograms. *Vis. Neurosci.* 14:73–82. <http://dx.doi.org/10.1017/S0952523800008774>
- Pugh, E.N. Jr., and T.D. Lamb. 1993. Amplification and kinetics of the activation steps in phototransduction. *Biochim. Biophys. Acta.* 1141:111–149. [http://dx.doi.org/10.1016/0005-2728\(93\)90038-H](http://dx.doi.org/10.1016/0005-2728(93)90038-H)
- Pugh, E.N. Jr., B. Falsini, and A. Lyubarsky. 1998. The origin of the major rod- and cone-driven components of the rodent electroretinogram and the effect of age and light-rearing history on the magnitude of these components. In *Photostasis and Related Phenomenon*. T. Williams and A.B. Thistle, editors. Springer US, New York. 93–128. http://dx.doi.org/10.1007/978-1-4899-1549-8_7
- Robson, J.G., and L.J. Frishman. 2014. The rod-driven a-wave of the dark-adapted mammalian electroretinogram. *Prog. Retin. Eye Res.* 39:1–22. <http://dx.doi.org/10.1016/j.preteyeres.2013.12.003>
- Sherry, D.M., A.R. Murray, Y. Kanan, K.L. Arbogast, R.A. Hamilton, S.J. Fliesler, M.E. Burns, K.L. Moore, and M.R. Al-Ubaidi. 2010. Lack of protein-tyrosine sulfation disrupts photoreceptor outer segment morphogenesis, retinal function and retinal anatomy. *Eur. J. Neurosci.* 32:1461–1472. <http://dx.doi.org/10.1111/j.1460-9568.2010.07431.x>
- Sokal, I., G. Hu, Y. Liang, M. Mao, T.G. Wensel, and K. Palczewski. 2003. Identification of protein kinase C isozymes responsible for the phosphorylation of photoreceptor-specific RGS9-1 at Ser475. *J. Biol. Chem.* 278:8316–8325. <http://dx.doi.org/10.1074/jbc.M211782200>
- Umino, Y., and E. Solessio. 2013. Loss of scotopic contrast sensitivity in the optomotor response of diabetic mice. *Invest. Ophthalmol. Vis. Sci.* 54:1536–1543. <http://dx.doi.org/10.1167/iops.12-10825>
- Umino, Y., E. Solessio, and R.B. Barlow. 2008. Speed, spatial, and temporal tuning of rod and cone vision in mouse. *J. Neurosci.* 28:189–198. <http://dx.doi.org/10.1523/JNEUROSCI.3551-07.2008>
- Umino, Y., R. Herrmann, C.K. Chen, R.B. Barlow, V.Y. Arshavsky, and E. Solessio. 2012. The relationship between slow photoresponse recovery rate and temporal resolution of vision. *J. Neurosci.* 32:14364–14373. <http://dx.doi.org/10.1523/JNEUROSCI.1296-12.2012>